Ministry of Higher Education

and Scientific Research

Journal of Kufa for Chemical Sciences

A refereed

Research Journal Chemical Sciences

Vol.2 No.9 Year 2022

ISSN 2077-2351

Synthesis, Characterization and evaluation of two organic compounds as corrosion inhibitors for carbon steel alloy (C1010) in acidic medium of 0.1M HCl.

Alhawraa. A. Alasadi [1، a)], Hadi Z. Al-Sawaad [2، b)], Ahmed A. AlWaaly[3، c)]

1,2,3University of Basra, College of Science, Department of Chemistry

a) *hadi.ziara@uobasrah.edu.iq* **b)** *ahmed.alwaaly@me.com*

*c)**alhawraa.muhsan.sci@uobasrah.ed***

الخلاصة:

في هذه الدراسة تم تحضيرالمركبان(D1) 4-chlorobenzodithioatebenzyltrimethylammonium و(D2) 4-methoxylbenzodithioatebenzyltrimethylammonium وتم تشخيص هذان المركبان بتقنيات H-NMR و FT-IR و UV-Visible و Mass. ثم تم تقييم المركبان كمثبطان في وسط تآكل حامضي من (0.1M) من حامض الهيدروكلوريك لتآكل سبيكة حديد الصلب الكربوني (C1010) عند 25^0C وأظهرالمركب D1 عند التركيز الامثل (9ppm) كفاءة تثبيط 97.91%، كما اظهرالمركب D2 عند التركيز الامثل (8ppm) كفاءة تثبيط 97.07% وتمت دراسة تأثير درجة الحرارة على سلوك المثبطان عند ^{0}C(55,45,33) ولكل مثبط على انفراد وتبين بارتفاع درجة الحرارة تنخفض قيمة كفاءة التثبيط ،و تم حساب الدوال الحركية مثل Ea و *ΔH و *ΔS و *ΔG . توضح ان التفاعل يكون ماص للحرارة بوجود المثبط وعدم وجوده وان كلا المثبطان يسلكان سلوك المثبط المزدوج.

Abstract

In this study, 4-chlorobenzodithioatebenzyltrimethylammonium and 4-methoxylbenzodithioatebenzyltrimethylammonium were synthesized and characterized by ^{1}H-NMR, FTIR, UV-Visible and Mass techniques. Then they evaluated as corrosion inhibitors for carbon steel alloy (C1010) against corrosive environment of hydrochloric acid at different concentrations at 25 ˚C. both inhibitors revealed an excellent inhibition efficiency (97.95) % and (97.13) % at optimal concentrations (9) ppm and (8) ppm respectively. The effect of temperature on the corrosion was studied in absence and presence of the inhibitor, the raising of temperature leads to reduce the efficiency of the inhibitor and CR was enhanced. On the other hand, kinetic parameters such as activation energyE_a^*, enthalpy of activationΔH^*, entropy of activation $\Delta S^*$and Gibbs free energy of activation ΔG^* were calculated which are insisted a physical adsorbed behavior for the inhibitor, an endothermic corrosion reaction whether in presence or in absence of the inhibitor and enhanced non-spontaneous behavior in presence of the certain inhibitor. Each one of the inhibitor has the mixed inhibition behavior.

1. Introduction

Corrosion is defined as the destruction of metals and alloys by the surrounding environment through chemical or electrochemical changes[1,47] . It is also known as a chemical or electrochemical oxidation process [2,3]. The study of corrosion is of great importance from an economic point of view, as it works to reduce direct and indirect economic losses, maintain the safety of operating tools and equipment, and preserve metallic materials. Corrosion inhibitors are defined as chemicals that are added in small quantities to reduce or prevent the rate of corrosion [40] because these materials have heterogeneous atoms (Sulfur, Nitrogen, Selenium, Phosphorous) [4]. These materials have the ability to adsorption. Chemically, physically, or both, the inhibitor may be in the form of vapor, liquid, or both[5,2] . Corrosion inhibitors work in the first step to transfer the inhibitor molecules or the so-called (inhibitor molecules) to the metal surface. In the next step, the active groups of the inhibitors interact with the metal surface, forming a protective layer on the metal surface, thus preventing the interaction of metals with the corrosive environment [2,6]. Corrosion is to be inhibited by organic compounds to be absorbed on the metal surface to form a protective The layer's act as insulators between the surface of the metal and amid corrosion [7,8].

Thiolate[48] compounds or what is known as mercaptans, they are organic compounds that contain a (sulfohydryl) SH group attached to a carbon atom. Thiols are similar to alcohols in that the oxygen atom in alcohols has been replaced by a sulfur atom (oxygen and sulfur have almost the same chemical properties because they belong to the same group). Alcohols and thiols share some similarities, which means that the sulfur prefixes are a larger component compared to oxygen, and the length of the (C-S) bond is greater than the (C-O) bond. The hydrogen bond between thiol groups is much weaker in liquids or solids mainly due to the strength of cohesion.

2. Material and Methods

2.1. Chemicals

The chemicals used in this study were purchased from various companies, including: Hydrochloric acid(37%Aldrich), Ethanol (99.99 %Scharlau), Di ethyl ether (99.5% SCH), n-hexane(97.0% Aldrich) ،4-methoxy phenyl Magnesium bromide solution (99.99%Aldrich) ،4-chloro phenyl Magnesium bromide solution(99.98%Aldrich، benzyltrimethylammoniumhydroxide(99.98%Aldrich).

2.2 Synthesis of4-chlorobenzodithioate benzyl tri methyl ammonium

A three necked round bottom flask (250) mL was charged by the solution of (4-chloro phenyl magnesium bromide [(0.016) mol dissolved in (16) mL THF], (0.016) mol of CS_2 solution was added, the reaction was stirring for (1.5) h then, after that a mixture of 72mL (11N), hexane (80) mL and ice (100) g were added to the reaction mixture under continuous stirring for (1) h. a reddish organic layer was extracted from the reaction solution then, (6.5) g of benzyl trimethyl ammoniumhydroxide was added and the reaction was started again under continuous stirring for (2)h. after that, the reaction is cooled down, the precipitate is filtered and washed by n-hexane and left to dry in the air[9]. After drying, the yield was (5.19 g). The reaction steps are shown in scheme 1 below:

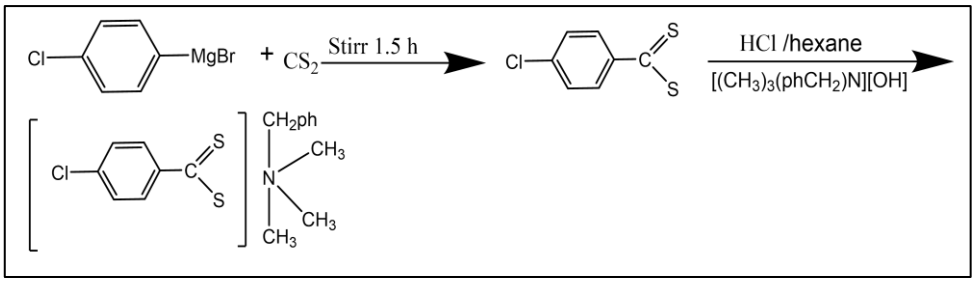

Scheme (1): Synthesis of D1.

Synthesis of 4-Methoxylbenzodithioic acid benzyl trimethylammonium (D2) was synthesized by the same procedure for synthesized D1 but, the quantities include (0.005) mol of methoxy phenyl magnesium bromide dissolved in (15) mL THF, CS2 (0.05) mol (3) mL, (0.005) methoxy phenyl magnesium bromide, (22.5) mL hydrochloric acid (11N), n-hexane (40) mL, ice (100 g) and (1.75) g of Benzyl trimethyl ammonium hydroxide. After drying, the yield was (3.5g). The reaction steps are summarized in scheme 2 below:

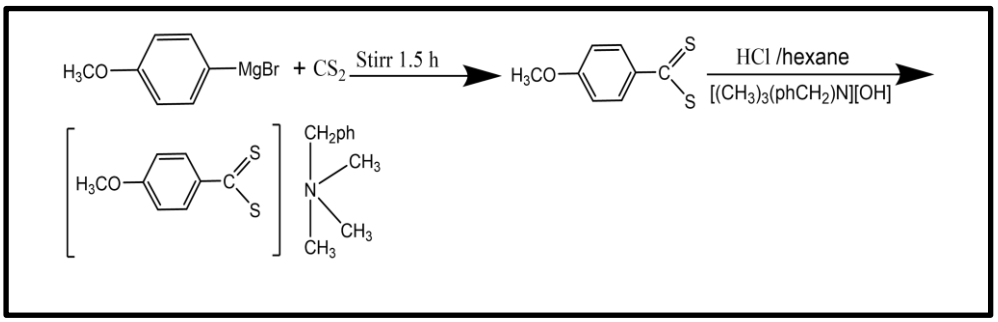

3. Characterization of the ligand D1 and ligand D2.

3.1. UV-Visible ligand D1 and ligand D2[10,11,12,13].

Bothe D1 and D2 compound were characterized by UV-Visible as shown in Figures 1 and 2 below:

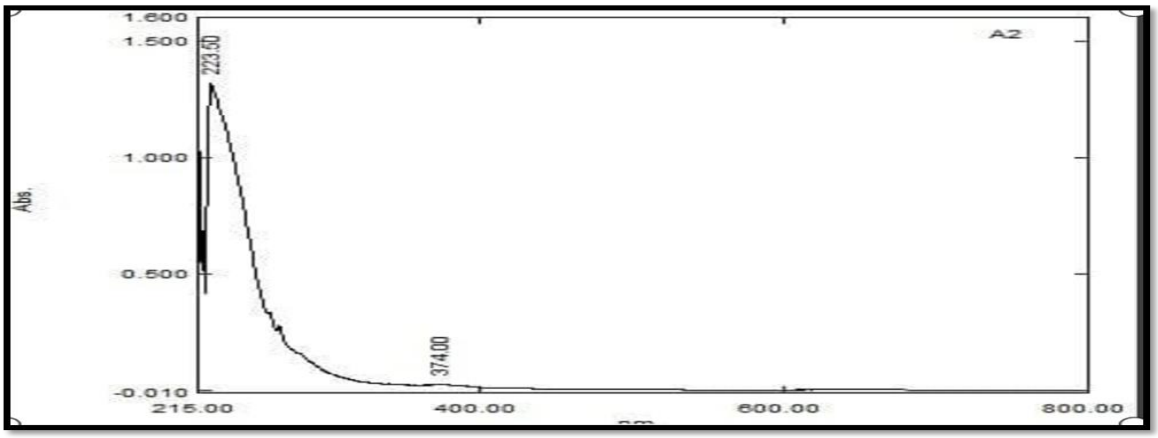

Figure 1: UV-Visible spectrum of D1

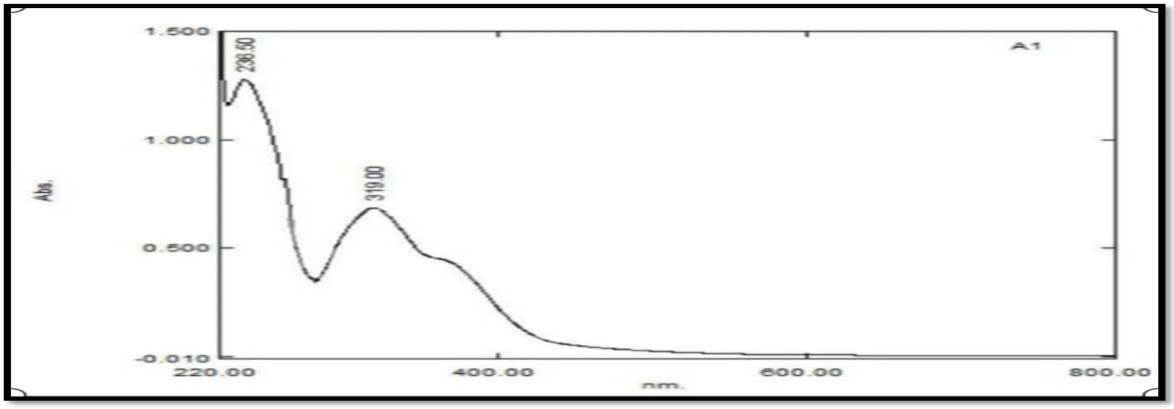

Figure 2: UV-Visible spectrum of D2

The possible electronic transitions are shown in the Table (1) below.

Table (1): The possible electronic transitions in D1 and D2 UV-Visible spectra.

Complex	Wavelength (nm)	Type of transition
D1	223.5 374	**π→π*** **n→π***
D2	236 319	**π→π*** **n→π***

Table 1 depicted the electronic transitions in both D1 and D2 compounds, $\pi \rightarrow \pi^*$ (223.5 and 236 nm for D1and D2 respectively.) While $n \rightarrow \pi^*$ at (374 and 319 nm for D1 and D2 respectively.) but $\pi \rightarrow \pi^*$ in D2 is greater than in D2 while the reverse in $n \rightarrow \pi^*$ this can be attributed to presence of methoxy group in D2 compared with chloro group in D1 make the resonance state in D2 greater than in case of D1 i.e., methoxy group raised the wavelength toward red shift in

$\pi \rightarrow \pi^*$ transition and blue shift in $n \rightarrow \pi^*$ transition in D2 compared with D1 [49].

3.2. FT-IR spectroscopy:

The two synthetic compoundsD1 and D2 are were characterized by FTIR technique [14,15,41] as KBr disc, as shown below in Figures 3 and 4respectively.

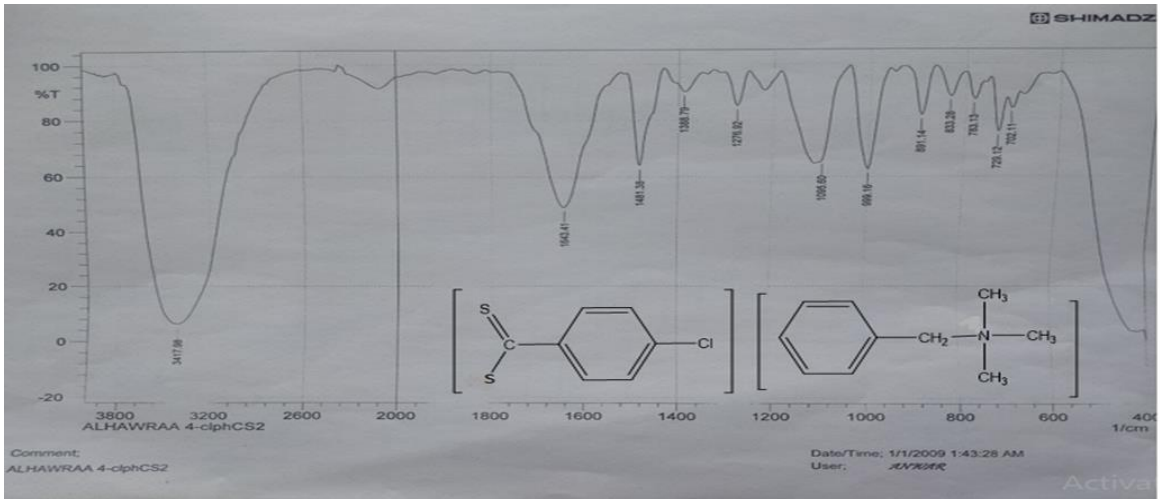

Figure 3: FT-IR spectrum for D1.

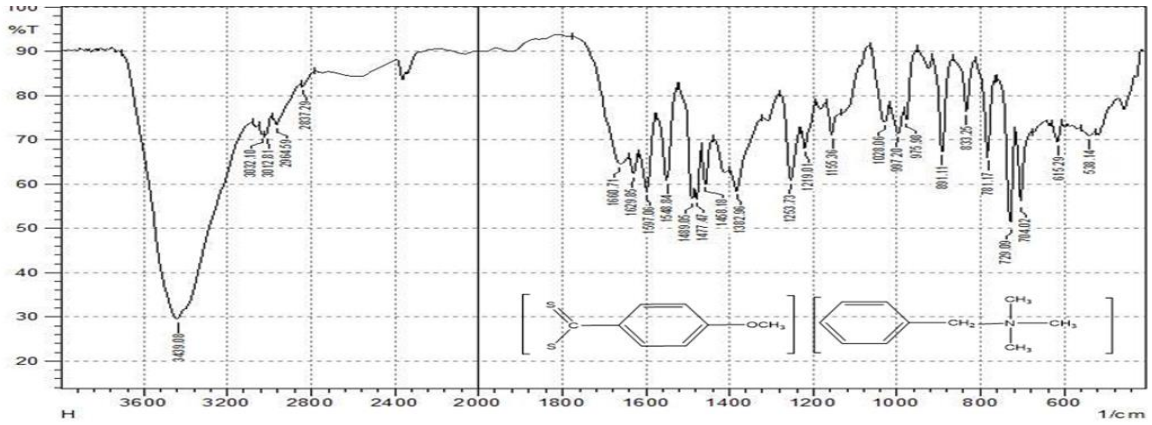

Figure 4: FT-IR spectrum for D2.

Figures 3 and 4 showed the important bands which are summarized in Table 2 below.

Table (2): The important FTIR bands for D1 and D2 compounds.

compound	C=C Str (Cm^{-1})	C-N (Cm^{-1})	C=S Str (Cm^{-1})	C-S (Cm^{-1})	C-O (Cm^{-1})	C-Cl (Cm^{-1})	C-H (Cm^{-1})
D1	1643	1276	1482	1095	-	702	3417
D2	1597	1253	asy 1489, sym 1477	asy 1253, sym 1219	asy1155, sym 1028	-	2964،*3012

* For aromatic ring. Asy=assymetric and sym=symmetric.

Table 2 depicted the obvious different in wave number values for FTIR spectra for D1 and D2. As shown above D1 at 702 Cm^{-1} assigned to C-Cl functional group which not found in D2 and vice versa, asy1155, sym 1028 bands are assigned to C-O functional group due to resonance between benzene ring with methoxy group in D2 that not found in D1[50,51]. The presence of asy and sym bands for C=S and C-S functional groups in D2 can be assigned for the same reason.

3.3. Mass spectra [16,17,18]:

According to mass spectrum of D1 in Figure 5 below, the suggested mechanism fragmentation for molecular ion 337 m/z with the molecular formula $[C17H20NS2Cl]^{+}$ obey to the following steps. The first decomposition depicted to loss of benzyl radical to form the molecular ion 246.1m/z to form the molecular formula $[C10H13NS2Cl]^{+}$ which decomposed to molecular ion 139 m/z with molecular formula [C5H4S2].+. the last decomposed to molecular ion 75m/z with molecular formula $[C6H3]^{+}$

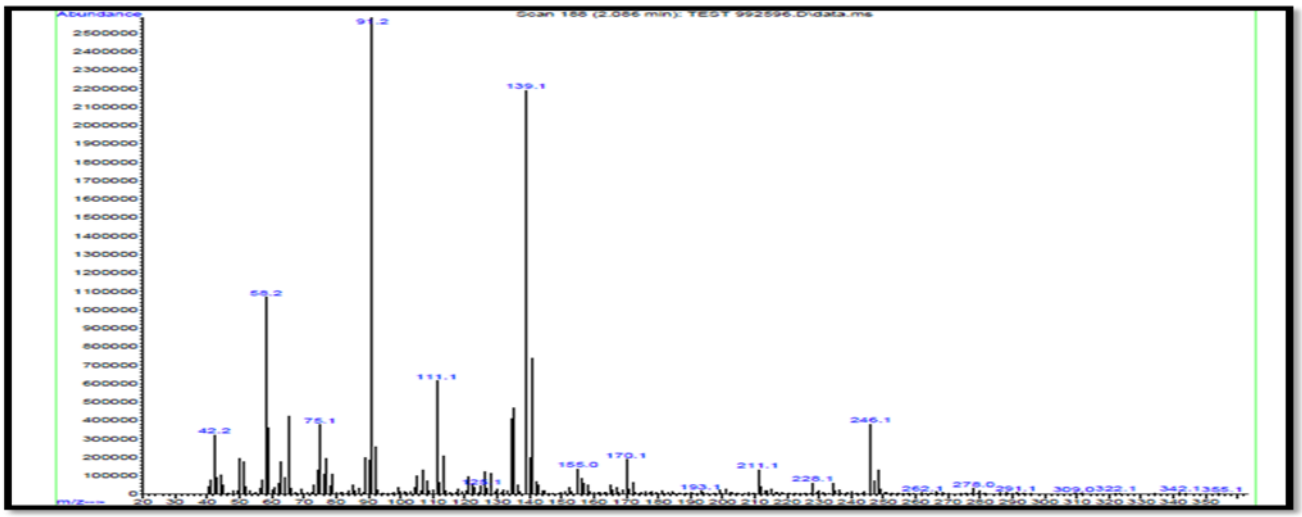

Figure 5: Mass spectrum for D1.

The mass spectrum for D2 as in Figure 6 reveals the molecular ion 333 m/z with molecular formula $[C18H23NOS2]^{+}$. This molecular ion decomposed as in the following suggested mechanism firstly into molecular ion 240 m/z with molecular formula $[C16H18NO]^{+}$ which decomposed into the molecular ion 135m/z with molecular formula $[C10H11N]^{+}$, after that the last molecular ion decomposed into molecular ion 91 m/z with molecular formula $[C7H7]^{+}$, the last decomposition includes loss of methylene group to for the molecular ion 77 m/z with molecular formula $[C6H7]^{+}$

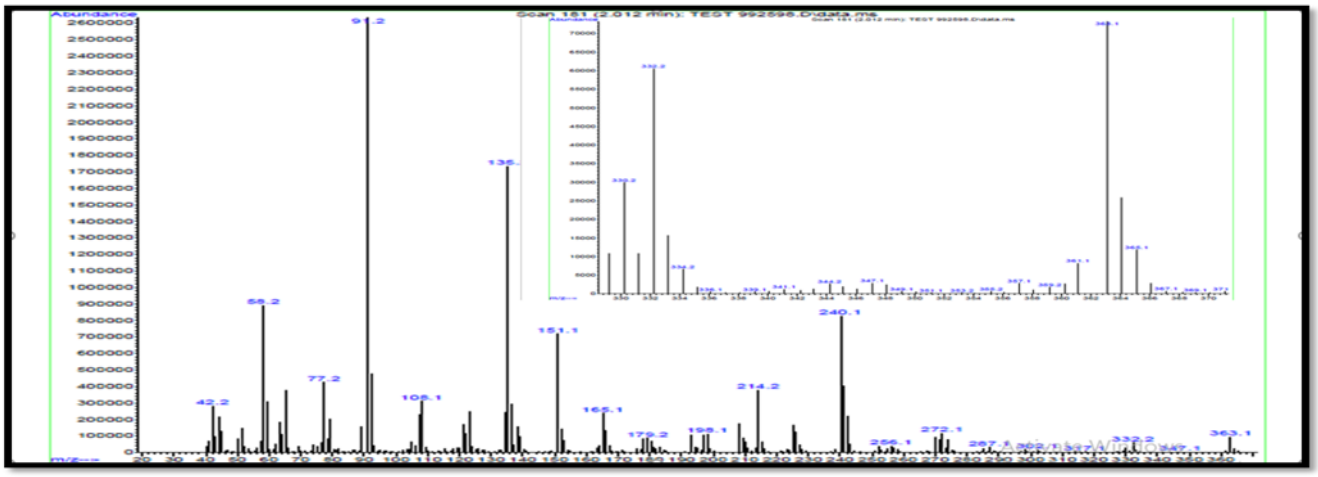

Figure 6: Mass spectrum for D2.

3.4. Nuclear magnetic resonance spectrum (H- NMR) [11,24,25,26]

D1 and D2 were characterized by 1HNMR as in Figures 7 and 8 below by dissolved each one of them in d^6DMSO as solvent. As shown in Figures 7 and 8, the signal with chemical shift 2.7ppm assigned to d^6DMSO [17,21]. The signals in Figure 7 can be assigned at chemical shifts (3.04-3.12) ppm to protons of the four methyl groups which attached with nitrogen atom, (4.34) ppm to protons of methylene group which lies between benzene ring and trimethylammonium ion, the chemical shift (6.46-7.11) ppm to the protons for benzene ring attached methylene group respectively. On the other hand, the protons of the second benzene ring that attached with chloro and CS2 have the chemical at range (7.26-8.07) ppm.

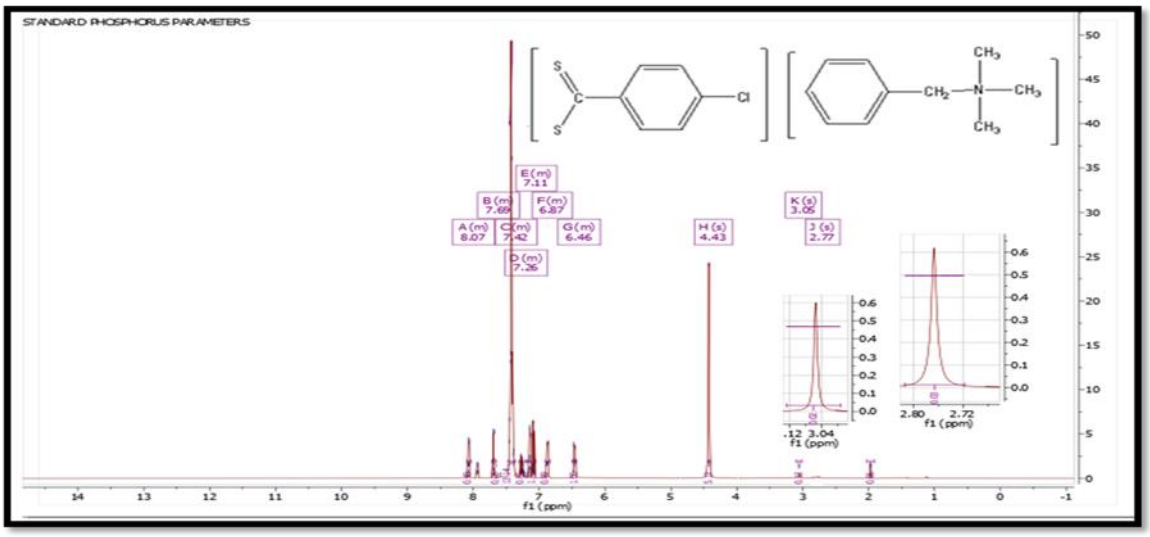

Figure 7: ^{1}H-NMR spectrum for D1.

Figure 8 below depicted 1HNMR signals with chemical shifts as follow, (3.86-3.90) ppm assigned to to protons of the four methyl groups which attached with nitrogen atom, (4.57) ppm to protons of methylene group which lies between benzene ring and trimethylammonium ion, the chemical shift (6.50-7.00) ppm to the protons for benzene ring attached methoxy group and CS2 group respectively. On the other hand, the protons of the second benzene ring that attached with quaternary ammonium ion have the chemical at range (7.50-8.50) ppm.

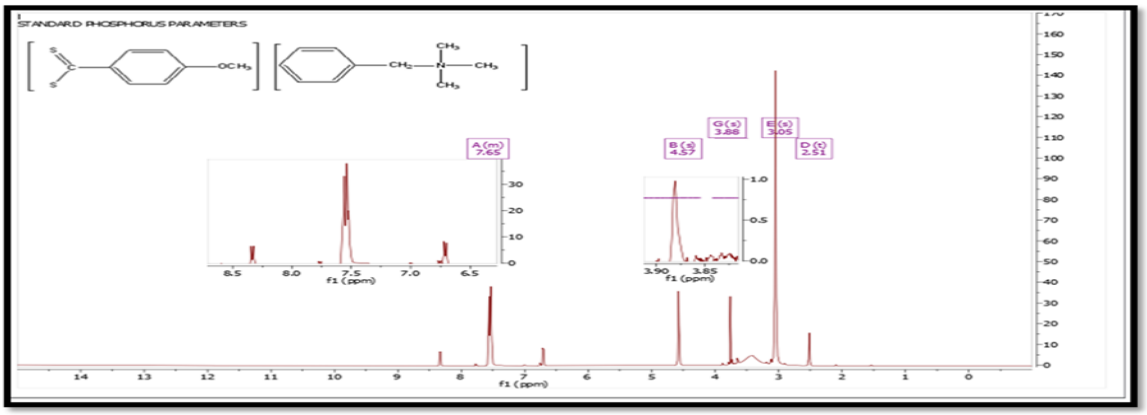

Figure 8: ^{1}H-NMR spectrum for D2.

4.Corrosion study:

In this study, D1 and D2 compounds were evaluated as corrosion inhibitors for the carbon steel alloy (C1010) by using the electrochemical methods (Tafel plots). The role of concentration of the inhibitor on the corrosion rate of the alloy at constant temperature (25°C) and the effect of the temperature on the inhibition efficiency of the certain inhibitor and the corrosion rate of the alloy were studied at temperature range (25˚C,35˚C,45˚C,55 ˚C). The constituents of the studied alloy are summarized in Table 3 below.

Table (3): Shows the components in the composition and proportions of carbon steel alloy.

Element	**C**	**Mn**	**Cr**	**P**	**S**	**Cu**	**Si**	**As**	**Ni**	**Fe**
w/w%	**0.13**	**0.30**	**0.10**	**0.05**	**0.04**	**0.30**	**0.37**	**0.08**	**0.30**	**Balance**

4.1. Preparation of working electrode.

The total subjected area to the corrosive environment for the studied alloy is 8.2426 Cm2 where, the dimensions for the strip's alloy include 3.2 Cm, 1.16 Cm and 0.16 Cm as length, width and thickness respectively. The strip was hanged through the hole with diameter 0.2Cm; these dimensions were measured by a

sensitive (1mm) Vernier scale. The alloy was polished by using silicon carbide paper with grades 400, 600, 880 and 1200 respectively then cleaned with shamawa cloth with alumina. The specimen washed by ethanol, by distilled water then greased and kept at desiccator with silica gel to protect the alloy from moisture.

4.2. Measurements [42,43]

The corrosion data were acquired through the apparatus consists of the following:

1. An electrochemical cell include the specimen alloy as Working Electrode (WE), platinum electrode as an Auxiliary Electrode (AE) and calomel electrode as reference electrode (RE). these electrodes were putted in Beaker with a capacity of 75 mL

2.The device is programmed by the following information including subjected area for the alloy to the corrosive environment whether in presence or absence of the inhibitor, the scan rate (10) $V.s^{-1}$, equivalent weight of alloy, the density of alloy and the range of scanning rate relative to open circuit potential (OCP) at range (+250) to (-250) mV.

5. Results and discussion:

Figures 9 and 10 depicted the Tafel plots curves for carbon steel alloy (C1010) in presences of certain concentrations from D1 and D2 respectively at constant temperature (25) ˚C temperature.

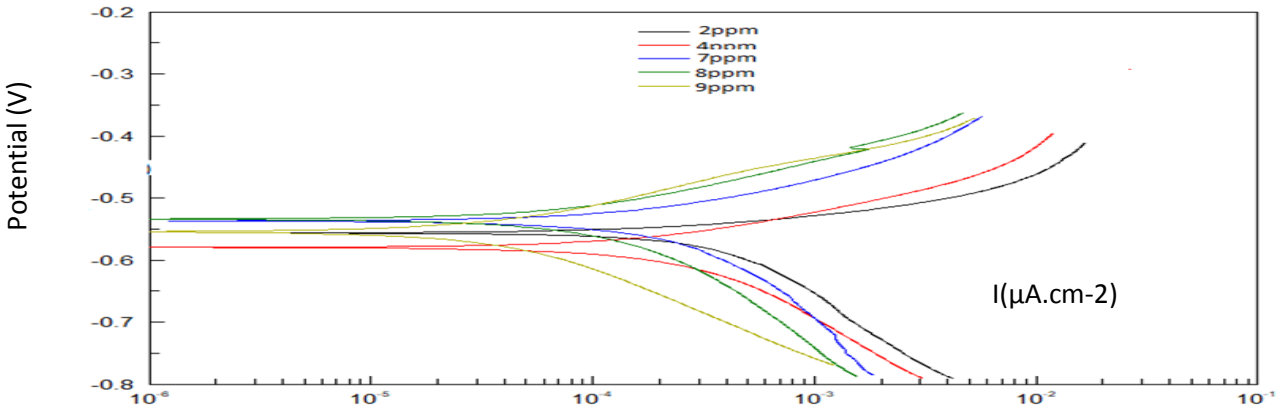

Figure (8): Tafel plot curves for alloy (C1010) in presence of different concentrations from D1 as corrosion

inhibitor at 25 ˚C.

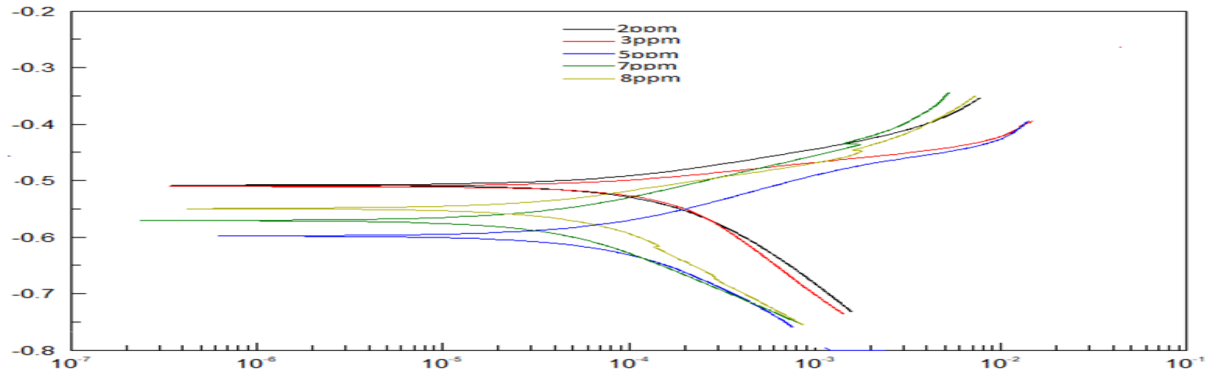

Figure (9): Tafel plot curves for alloy (C1010) in presence of different concentrations from D2 as corrosion inhibitor at 25 ˚C.

Moreover, the data which acquired from Tafel curves in above were summarized in Table 4 below.

Table (4): The electrochemical data for carbon steel in presence and absence of certain inhibitors against of corrosive environment of 0.1M from HCl at (25˚C).

Comp.	Conc. ppm	E_{corr} mV	β_a mV.decade^{-1}	β_c mV.decade^{-1}	R_p Ω.Cm^2	I_{corr} µA.Cm^{-2}	CR mpy	Effe. %	θ
HCl	3650	-567	213	-119.8	20.89	1596	738.49	-	-
D1	2	-558	94.86	-589.7	434.98	363.48	168.29	77.21	0.7721
	4	-580	93.05	-201.86	416.35	173.22	80.20	89.14	0.8914
	7	-537	116.32	-293.04	254.90	142.03	65.76	91.10	0.9110
	8	-534	102.68	-204.41	405.74	73.24	33.91	95.41	0.9541
	9	-555	85.319	-141.59	1611.68	32.76	15.17	97.95	0.9795
D2	2	-508	80.72	-203.11	405.61	173.95	80.54	89.10	0.8910
	3	-512	65.99	-308.64	637.45	143.43	66.41	91.01	0.9101
	5	-598	92.28	-150.53	1012.58	57.77	26.75	96.38	0.9638
	7	-530	75.64	-102.63	623.66	63.00	29.17	96.05	0.9605
	8	-550	77.21	-184.39	1413.29	45.79	21.20	97.13	0.9713

Inhibition efficiency for the inhibitor was calculated related to the following equation (1), [14,42,43]:

$$effeciency\% = \frac{CR_{uninhib} - CR_{inhib}}{CR_{uninhib}} \times 100 \quad \ldots\ldots 1$$

From Table 4 the presence of D1 or D2 as inhibitors against the corrosive 0.1M of hydrochloric acid suppressed the corrosion rate (CR) which attributed to reduce the corrosion current density (I_{corr}) that raised the resistance polarization(Rp) on the surface of alloy. Hence, as the concentration of the certain inhibitor (D1 or D2) increased, CR and I_{corr} were reduced while Rp values were raised. Moreover, the inhibition efficiency (Effeci. %) and surface coverage area (θ) were raised as concentration of the certain inhibitor increased, this can be attributed to increase the adsorbed film of the inhibitor on the surface of the alloy and the corrosive acid molecule will be ejected from the surface of alloy inhibition [14,15,41,50,21,44] .On the other hand, it will be noticed that the effect of chemical structure on the inhibition efficiency is obvious where, in all concentrations of D2 as inhibitor, the efficiency of inhibition is greater than in case of D1 inhibitor this is may be due to presence of methoxy group (electro with donating group) in D2 instead of chloro group (electron withdrawing) in D1 made the last inhibitor lesser efficiency than the first [21,44] .E_{corr} for the alloy in presence of D1 or D2 at the studied concentrations reveals a mixed inhibition behavior where the difference between E_{corr} values in presence of certain inhibitor and E_{corr} value in absence of the inhibitor is lesser than ±89mV [22]. Anodic Tafel constants ($\beta_{a)}$ and cathodic Tafel constants (β_c) on the other hand, revealed a simple blocking reaction sites whether in case of the studied concentrations of D1 or D2. [23]

5.2. The effect of temperature on inhibition efficiency at optimal concentration.

The effect of temperature on the corrosion rate for the carbon steel alloy in absence, presence of the certain inhibitors and on the inhibition efficiency for the synthetic inhibitors at optimal concentration were achieved at temperature range of (298-328) K (25-55) ˚C. Table (5) shows the acquired electrochemical data from Tafel plot curves at this range of temperatures which showed at Figures 10, 11 and 12 respectively.

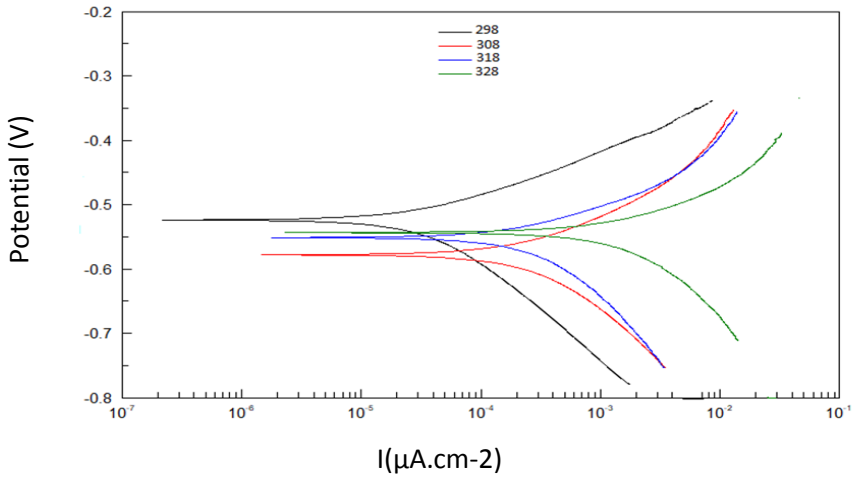

Figure (10): Tafel plot curves for alloy (C1010) carbon steel iron in presence of corrosive environment (0.1M HCl) at different temperatures.

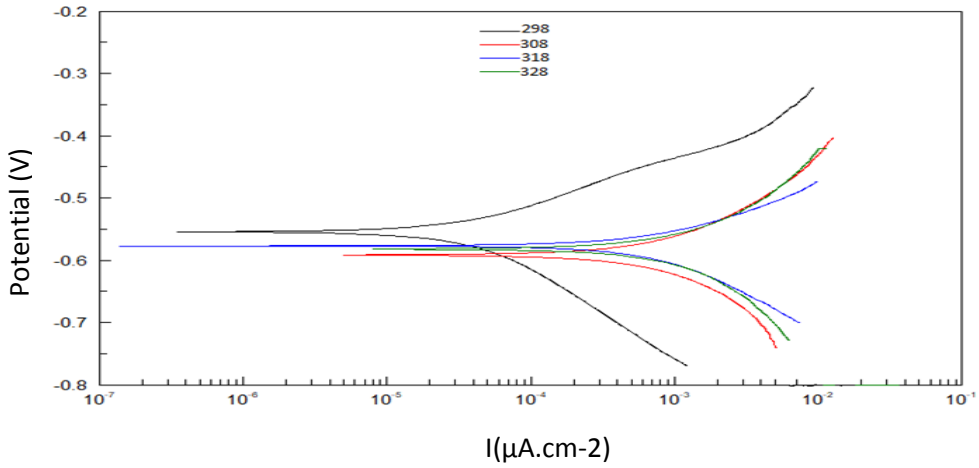

Figure (11): Tafel plot curves for alloy (C1010) carbon steel in presence of optimal concentration (9ppm) of D1 inhibitor against the corrosive environment of (0.1M HCl) atdifferent temperatures.

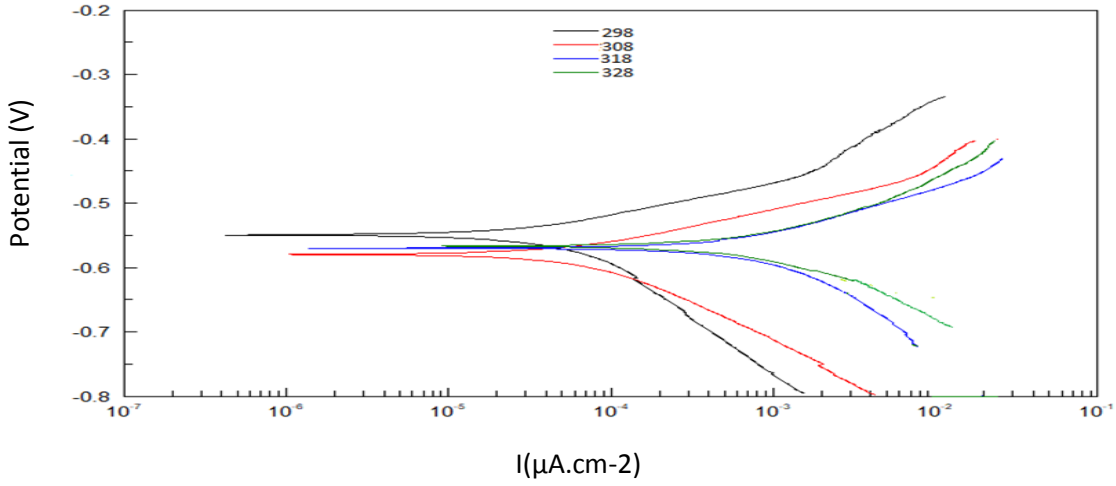

Figure (12): Tafel plot curves for alloy (C1010) carbon steel in presence of optimal concentration (8ppm) of D2 inhibitor against the corrosive environment of (0.1M HCl) at different temperatures.

Table (5): Electrochemical results obtained from the temperature effect of the C1010 method with inhibitors at the greatest concentration within the thermal range (298-328K) (25-55) C0.

Comp.	Conc. ppm	Temp. K	E_{corr} mV	β_a mV.decade^{-1}	β_c mV.decade^{-1}	R_p Ω.Cm^2	I_{corr}. µA.Cm^{-2}	C_R mpy	Effe. %	θ
HCl	3650	298	-567	213.00	-119.80	20.89	1596.0	738.49	-	-
HCl		308	-578	108.00	-161.00	14.60	1925.0	891.28	-	-
HCl		313	-552	97.61	-202.00	33.82	2151.5	996.14	-	-
HCl		328	-544	118.49	-205.00	11.79	5340	2472.42	-	-
D1	9	298	-555	85.319	-141.59	1611.68	32.76	15.17	97.95	0.9795
	9	308	-591	188.14	-249.00	81.31	573.07	265.33	70.23	0.7023
	9	313	-577	133.86	-161.00	48.88	650.08	300.98	69.79	0.6979
	9	328	-582	237.00	-335.00	82.58	730.81	338.37	86.13	0.8613
D2	8	298	-550	77.21	-184.39	1413.29	45.79	21.20	97.13	0.9713
	8	308	-580	63.57	-119.00	570.21	76.43	35.39	96.03	0.9603
	8	313	-569	97.68	-162.00	86.73	696.57	322.51	67.62	0.6762
	8	328	-566	131.05	-243.00	49.77	743.76	344.36	86.07	0.8607

Table 5 reveals that as temperature raised, Rp, efficiency and θ values were suppressed due to the increasing Icorr and in turn CR values respectively because of the dissolving of the adsorbed inhibitor's film for the certain inhibitor [24,25].

5.2. Corrosion kinetic study

The kinetic for the corrosion reaction was studied in absence and presence of the optimal concentration of the certain inhibitor. Thus, kinetic parameters such as an activation energy E_a^*, enthalpy of activation ΔH^*, entropy of activation $\Delta S^*$and Gibbs free energy of activation ΔG^* , firstly an activation energy E_a^* is calculated according to Arrhenius equationas[45,46,26,27] in equation 2 below:

$$\ln CR = \ln A - \frac{E_a^*}{RT} \quad \text{.....2}$$

Where, E_a^* is an activation energy in kJ.mol^{-1}, A in s^{-1} is an Arrhenius pre-exponential, R is the universal gas which equal to $8.314\, J.K^{-1}.mol^{-1}$ and T is the absolute temperature in K. by plotting ln CR against 1/T , the slope is $\frac{E_a^*}{R}$ and the intercept is ln A as in Figure 13 below:

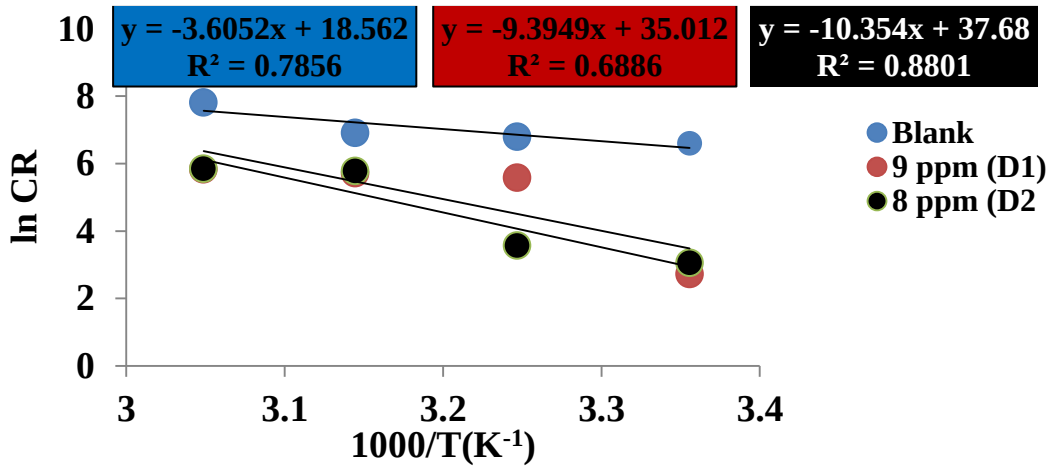

Figure (13): Arrhenius relationship plot to calculate the activation energy in absence and presence of the certain inhibitor at its optimal concentration. In order to calculate the enthalpy of activation ΔH* and entropy of activation ΔS*, equation 2 below [28,29,30] was used by plotting the relationship between $\ln\frac{CR}{T}$ against $\frac{1}{T}$. Thus, slope equal to $\frac{-\Delta H^*}{R}$ and the intercept is $[\ln\frac{R}{Nh}+\frac{\Delta S^*}{R}]$ as in Figure 14 below:

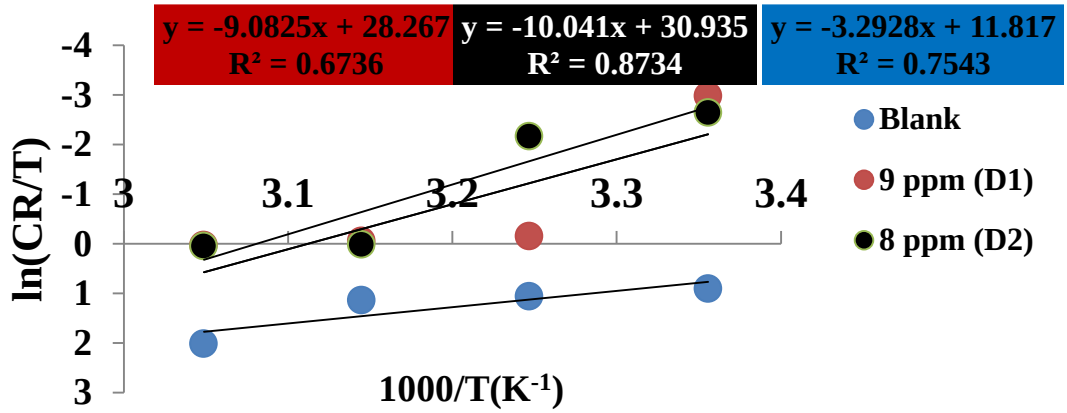

Figure (14): Calculation of the activation enthalpy and activation entropy in absence and presence of the certain inhibitor at its optimal concentration.

$$\ln\frac{CR}{T}=\ln\frac{R}{Nh}+\frac{\Delta S^*}{R}]\frac{-\Delta H^*}{RT} \quad \ldots\ldots (3)$$

Where N is Avocado's number ($6.023\times10^{23}mol^{-1}$), h is Plank's constant ($6.625\times10^{-34}J.s$). Moreover, Gibbs's free energy of activation is calculated according to the following equation:

$$\Delta G^*=\Delta H^*-T\Delta S^* \quad \ldots\ldots (4)$$

The data which acquired from the equations 2,3 and 4 are tabulated in Table 6 below:

Table (6): Kinetic parameters for the corrosion reaction of carbon steel alloy in absence and presence of optimal concentration of the inhibitor.

Conc.	Conc. ppm	E_a^* kJ.mol^{-1}	A s^{-1}	ΔH^* kJ.mol^{-1}	ΔS^* J.mol^{-1}.K^{-1}	ΔG^* kJ.mol^{-1}
HCl	3650	29.97	1.15×10^8	27.38	-99.29	56.97
D1	9	78.11	1.61×10^{15}	75.51	37.47	64.34
D2	8	86.08	2.31×10^{16}	83.48	59.65	65.70

As shown from Table (6) above, the activation of energy for the corrosion reaction of alloy in absence of any inhibitor is relatively low which raised in presence of whether D1 or D2 which insisted that presence of the inhibitor was reduced the corrosion reaction this can be attributed to raise the energy barrier for the corrosion reaction in presence of inhibitor compared with the absence[31,32], especially in presence of D2 it may be because in D2 methoxy group will enhanced the inhibition effect compared with chloro group in D2[33]. The activation of energy value in presence of inhibitor D1 or D2 is lesser than 100kJ.mol-1 insisted that both of them physically adsorbed on the surface of alloy [34].

On the other hand, the enthalpy of activation values for the corrosion reaction depicted an endothermic behavior in absence and presence of the certain inhibitors which raised in presence of the inhibitor compared with the absence, this fact corresponded with enhance the CR, reduce in Rp and efficiency% values [35]as temperature raised in Table 5. Entropy of activation value in absence of the inhibitor is negative which refers to stabilize the corrosion product on the surface of alloy while in presence of the inhibitor D1 or D2 on the surface of alloy make the entropy of activation is positive this can be attributed to tends the adsorbed of inhibitor's molecules to make an activation complex on the surface of alloy with corrosion products as rate determining step [36,37] ،Gibbs free energy of activation as in Table 6 are positive value which raised in presence of the inhibitor D1 or D2 i.e., the nonspontaneous behavior is enhanced in presence of the inhibitor [38,39].

Conclusions

Both D1 and D2 are an excellent inhibitor against the acidic corrosive medium of 0.1M from HCl with inhibition efficiencies 97.95% and 97.13% respectively. The role of each one of them is raised the Rp values, reduce I_{corr} and

CR values. These inhibitors behave as mixed inhibitors with simple blocking reaction behavior. Each one of them is physically adsorbed on the surface of alloy. The increasing of the concentration of the inhibitor raised the inhibition efficiency whereas the optimal concentration of the inhibitors D1 and D2 are 9 ppm and 8 ppm respectively. When temperature is raised, the inhibition efficiency was suppressed and CR was raised. An activation energy of corrosion reaction was raised in presence of the inhibitor and the non-spontaneous of the reaction was increased in addition to the endothermic behavior for the reaction was enhanced in presence of the inhibitor compared with the absence.

References

1. Lebrini M, Robert F, Roos C. Adsorption properties and inhibition of C38steel corrosion in hydrochloric solution by some indole derivates: temperature175 effect, activation energies, and thermodynamics of adsorption. International Journal of corrosion. 2013; p 1-12

2. Raja, P. B.; Ismail, M.; Ghoreishiamiri, S.; Mirza, J.; Ismail, M. C.; Kakooei, S.; Rahim, A. A., Reviews on corrosion inhibitors: a short view. Chemical Engineering Communications 2016, 203 (9), 1145-1156.

3. Amer, B.; Abdel-Aziz, M.; El-Ashtoukhy, E.-S.; Amin, N., Galvanic Corrosion of Steel in Agitated Vessels Used in Fertilizer Industry. Theoretical Foundations of Chemical Engineering 2019, 53 (2), 280-291.

4. Izionworu, V.; Ukpaka, C.; Oguzie, E., Green and eco-benign corrosion inhibition agents: Alternatives and options to chemical based toxic corrosion inhibitors. Chemistry International 2020, 6 (4), 232-259.

5. Raja, P. B.; Sethuraman, M. G., Natural products as corrosion inhibitor for metals in corrosive media—a review. Materials letters 2008, 62 (1), 113-116.

6. Alhijaj, H. A. A. Synthesis and Characterization of Polymeric Compounds from Waste Polyethylene Terephthalate and Polystyrene and studying its Efficiencies as Oil Spill Cleanup and Corrosion Inhibitors, Ph.D. thesis, University of Basrah, 2015.

7. Fawzy, A., Zaafarany, I.A., Ali, H.M., and Abdallah, M., New synthesized amino acids-based surfactants as efficient inhibitors for corrosion of mild steel in hydrochloric acid medium: kinetics and thermodynamic approach, Int. J. Electrochem. Sci., 2018, vol. 13, no. 5, p. 4575.

8.Hazazi, O., Fawzy, A., and Awad, M., Synergistic effect of halides on the corrosion inhibition of mild steel in H2SO4 by a triazole derivative: kinetics and thermodynamic studies, Int. J. Electrochem. Sci., 2014, vol. 9, p. 4086.

9. Nucleophilic Substitution by Benzodithioate Anions, Chantal Bonnans-Plaisance and Jean-Claude Gressiw.

10. Samarasinghe, W.; Sithambaresan, M.; Mahendranathan, C., Synthesis, Characterization and Evaluation of Antibacterial Activity of a New Phenylmethylidene Thiourea Derivative and Its Copper (II) Complex. International Journal of Current Innovations in Advanced Research 2018, 1 (4), 59-68.
11. Sonmez, M., Synthesis and characterization of copper (II), nickel (II), cadmium (II), cobalt (II) and zinc (II) complexes with 2-benzoyl-3-hydroxy-1-naphthylamino-3-phenyl-2-propen-1-on. Turkish Journal of Chemistry 2001, 25 (2), 181-186.
12. Zakaria, S. A.; Muharam, S. H.; Yusof, M. S. M.; Khairul, W. M.; Kadir, M. A.; Yamin, B. M., Spectroscopic and structural study of a series of pivaloylthioderivatives. Malaysian Journal of Analytical Sciences 2011, 15 (1), 37-45.
13. Refat, M. S.; El-Deen, I. M.; Zein, M. A.; Adam, A. M. A.; Kobeasy, M. I., Spectroscopic, structural and electrical conductivity studies of Co (II), Ni (II) and Cu (II) complexes derived from 4-acetylpyridine with thiosemicarbazide. International Journal of Electrochemical Science 2013, 8 (7), 9894-9917.
14. O.B. Ibrahim, Complexes of urea with Mn (II), Fe (III), Co (II), and Cu (II) metal ions. Advances in Applied Science Research, 3(6) (2012) 18.
15. K.G. Akpomie, O.M. Famyomi, C.C. Ezeofor, R.S. Ato, W.E.V. Zyl, Insights into the use of metal complexes of thio derivatives as highly efficient adsorbents for ciprofloxacin from contaminated water. Transactions of the Royal Society of South Africa, 74(2) (2019) 180-188.
16. Binzet, G.; Kavak, G.; Külcü, N.; Özbey, S.; Flörke, U.; Arslan, H., Synthesis and characterization of novel thiourea derivatives and their nickel and copper complexes. Journal of Chemistry 2013, 2013.
17. Ghazal, K.; Shoaib, S.; Khan, M.; Khan, S.; Rauf, M. K.; Khan, N.; Badshah, A.; Tahir, M. N.; Ali, I., Synthesis, characterization, X-ray diffraction study, in-vitro cytotoxicity, antibacterial and antifungal activities of nickel (II) and copper (II) complexes with acyl thiourea ligand. Journal of Molecular Structure 2019, 1177, 124-130.
18. Arslan, H.; Duran, N.; Borekci, G.; Koray Ozer, C.; Akbay, C., Antimicrobial activity of some thioderivatives and their nickel and copper complexes. Molecules 2009, 14 (1), 519-527.
19. Samarasinghe, W.; Sithambaresan, M.; Mahendranathan, C., Synthesis, Characterization and Evaluation of Antibacterial Activity of a New Phenylmethylidene Thiourea Derivative and Its Copper (II) Complex. International Journal of Current Innovations in Advanced Research 2018, 1 (4), 59-68.

20. NAZIR, U., et al. Biferrocenyl Schiff bases as efficient corrosion inhibitors for an aluminium alloy in HCl solution: a combined experimental and theoretical study. RSC Advances, 2020, 10.13: 7585-7599.
21. Ali A. Naser1, Hadi Z Al-Sawaad2, Alaa S. Al-Mubarak3 Novel graphene oxide functionalization by urea and thiourea, and their applications as anticorrosive agents for carbon steel alloy in acidic medium.2020, Volume 11, Issue 3, Page 404-420.
22. Israa M. Al-Jubanawi, Hadi Z. Al-Sawaad, Ahmed A. AlWaaly 3 Bis thiourea phthalato Cobalt (Ⅱ) complex: synthesis and studying as corrosion inhibitors for carbon steel alloy(C1010) in 0.1M HCl J. Mater. Environ. Sci., 2020, Volume 11, Issue 8, Page 1386-1402.
23. Al – Sawaad. H.Z. (2013). Evaluation of the ceftriaxone as corrosion inhibitor for carbon steel alloy in 0.5 M of hydrochloric acid. Int. J. Electrochem. Sci,8, P 3105-3120.
24. Badertscher, M.; Bühlmann, P.; Pretsch, E., Structure Determination of Organic Compounds: Tables of Spectral Data. Springer: 2009.
25. Gurudatt, D. M.; Mohana, K. N. S., Influence of some synthesized pyrimidine derivatives on corrosion inhibition of mild steel in hydrochloric acid medium. European Journal of Chemistry 2014, 5 (1), 53-64.
26. Khadom, A. A., EFFECT OF TEMPERATURE ON CORROSION INHIBITION OF COPPER-NICKEL ALLOY BY TETRAETHYLENEPENTAMINE UNDER FLOW CONDITIONS. Journal of the Chilean Chemical Society 2014, 59 (3), 2545-2549.
27. Mohammed Ali Al-Sammarraie, A.; Hasan Raheema, M., Electrodeposited reduced graphene oxide films on stainless steel, copper, and aluminum for corrosion protection enhancement. International Journal of Corrosion 2017, 2017.
28. Rao, S. A.; Rao, P., Corrosion inhibition and adsorption behavior of Murraya koenigii extract for corrosion control of aluminum in hydrochloric acid medium. Surface Engineering and Applied Electrochemistry 2017, 53 (5), 475-485.
29. Kairi, N. I.; Kassim, J., The effect of temperature on the corrosion inhibition of mild steel in 1 M HCl solution by Curcuma longa extract. International Journal of Electrochemical Science 2013, 8 (5), 7138-7155.
30. Dohare, P.; Quraishi, M.; Obot, I., A combined electrochemical and theoretical study of pyridine-based Schiff bases as novel corrosion inhibitors for mild steel in hydrochloric acid medium. Journal of Chemical Sciences 2018, 130 (1), 8.
31. Al-Sawaad, H. Z.; Faili, N. T.; Essa, A. H., Evaluation of Vicine as a Corrosion Inhibitor for Carbon Steel Alloy. Portugaliae Electrochimica Acta 2019, 37 (4),

205-216.
32. El-Tabesh, R.; Abdel-Gaber, A.; Hammud, H.; Oweini, R., Effect of Mixed-Ligands Copper Complex on the Corrosion Inhibition of Carbon Steel in Sulfuric Acid Solution. Journal of Bio-and Tribo-Corrosion 2020, 6 (2),
33. Dave, P.; LV, C., Schiff based corrosion inhibitors for metals in acidic environment: A reviewe. Material Sci & Eng 2018, 2 (6), 258-267.
34. Alhijaj, H. A. A. Synthesis and Characterization of Polymeric Compounds from Waste Polyethylene Terephthalate and Polystyrene and studying its Efficiencies as Oil Spill Cleanup and Corrosion Inhibitors, Ph.D. thesis, University of Basrah, 2015.
35. Larouj, M.; Ourrak, K.; El M'Rabet, M.; Zarrok, H.; Serrar, H.; Boudalia, M.; Boukhriss, S.; Warad, I.; Oudda, H.; Touir, R., Thermodynamic study of corrosion inhibition of carbon steel in acidic solution by new pyrimidothiazine derivative. J Mater Environ Sci 2017, 8 (11), 3921-3931.
36. Kairi, N. I.; Kassim, J., The effect of temperature on the corrosion inhibition of mild steel in 1 M HCl solution by Curcuma longa extract. International Journal of Electrochemical Science 2013, 8 (5), 7138-7155.
37. Dahdele, J.; Danaee, I.; Rashed, G., THERMODYNAMIC AND ADSORPTION ISOTHERM OF N, N'-BIS (2, 4, 6-TRIHYDROXYACETOPHENONE)-2, 2-DIMETHYLPROPANDIIMINE AS A CORROSION INHIBITOR ON SA-210 STEEL IN ALKALINE NACL SOLUTION. Journal of the Chilean Chemical Society 2016, 61 (3), 3025-3030.
38. Eddy, N. O.; Ameh, P. O.; Essien, N. B., Experimental and computational chemistry studies on the inhibition of aluminium and mild steel in 0.1 M HCl by 3-nitrobenzoic acid. Journal of Taibah University for Science 2018, 12 (5), 545-556.
39. Akinbulumo, O. A.; Odejobi, O. J.; Odekanle, E. L., Thermodynamics and adsorption study of the corrosion inhibition of mild steel by Euphorbia heterophylla L. extract in 1.5 M HCl. Results in Materials 2020, 5, 100074**.**
40. Al-Sawaad, H. Z. M. Preparation, Characterization, and Studying of Some of New Amino Resins as Corrosion Inhibitors for Carbon Steel and Brass Alloys, Ph.D. thesis, University of Basrah, 2009.
41. Radey, H. H. Synthesis, Characterization of Some graphene oxide derivatives and their Corrosion Inhibitor ability for carbon Steel in Acidic media, Ph.D. thesis, University of Basrah,2018
42. Faili, N. T. Plant Extraction and Natural Polymers Modification as Corrosion Inhibitors for N80 Steel in Acidic Media, Ph.D. thesis, University of Basrah, 2015.
43. Al-Sawaad, H. Z. M. Preparation, Characterization, and Studying of Some of

New Amino Resins as Corrosion Inhibitors for Carbon Steel and Brass Alloys, Ph.D. thesis, University of Basrah, 2009.
44.Biophysical study of some effective compounds Extracted from Laurus nobilis L, A Thesis submitted to in Partial Fulfillment of the Requirements of the degree of master of science in chemistry .**2021**
45. Israa Mohsin Mezaal, Synthesis, Characterization of Some New Thiourea, Phthalic Complexes of Fe(III), Co(II), Ni(II), and Cu(II) and Evaluation Them as Corrosion Inhibitors for Carbon Steel Alloy (C1010) Against Hydrochloric acid and Studying of their Electrical Conductivities, A thesis for the Degree of Master in Chemistry,2020.
46. Abbood, A. A.-A. Evaluation and Theoretical Study for Some Aminodiphosphonic Acids Derivatives as Corrosion and Scale Inhibiter for Mild Steel and Brass alloys in Aqueous Environments, Ph.D. thesis University of Basrah, 2016.
47. Kaesche H. Corrosion of metals: physicochemical principles and current problems: Springer Science & Business Media; 2012.
48. Organic Chemistry a Short Course, 13 Edition David J. Hart Christopher M. Hadad و Leslie E. Craine Harold Hart.
49.Spectrometric Identification of Organic Compounds, Robert M. Silverstein، Francis. Webster, David J. Kiemle, State University of New York, College of Environmental Science &Forestry.
50. Practical organic chemistry written by Dr. Hanan Abdel Jalil Radi and Dr. Muhammad Ahmed Abd. University of Basra, Department of Chemistry**.**
51. Spectral analysis using infrared rays, written by Dr. Abdel Alim Suleiman Abu Al-Majd.